

Imaging Mass Cytometry Identifies Structural and Cellular Composition of the Mouse Tissue Microenvironment

Kyle Driscoll, Qanber Raza, Michael Cohen, Smriti Kala, Liang Lim, Geneve Awong, Andrew Quong, Christina Loh
Standard BioTools Canada Inc., Markham, Ontario, Canada



Abstract

To demonstrate the capability of the IMC and single-cell analysis workflow for assessing mouse tissue microenvironment, we selected lung, an immune and vascular cell-ribose-rich tissue, for in-depth analysis. Our analysis identified the expression pattern of cellular markers as well as the localization of immune, epithelial, and stromal cell subpopulations. We demonstrate the broad applicability of our catalog antibodies on a variety of distinct mouse tissues such as bladder, kidney, salivary gland, small intestine, and testes. Furthermore, we classified the activation state of lymphoid and myeloid cell populations in the spleen, adhesion state of epithelial cells in the prostate, and molecular composition of the extracellular matrix in prostate, uterus, and kidney.

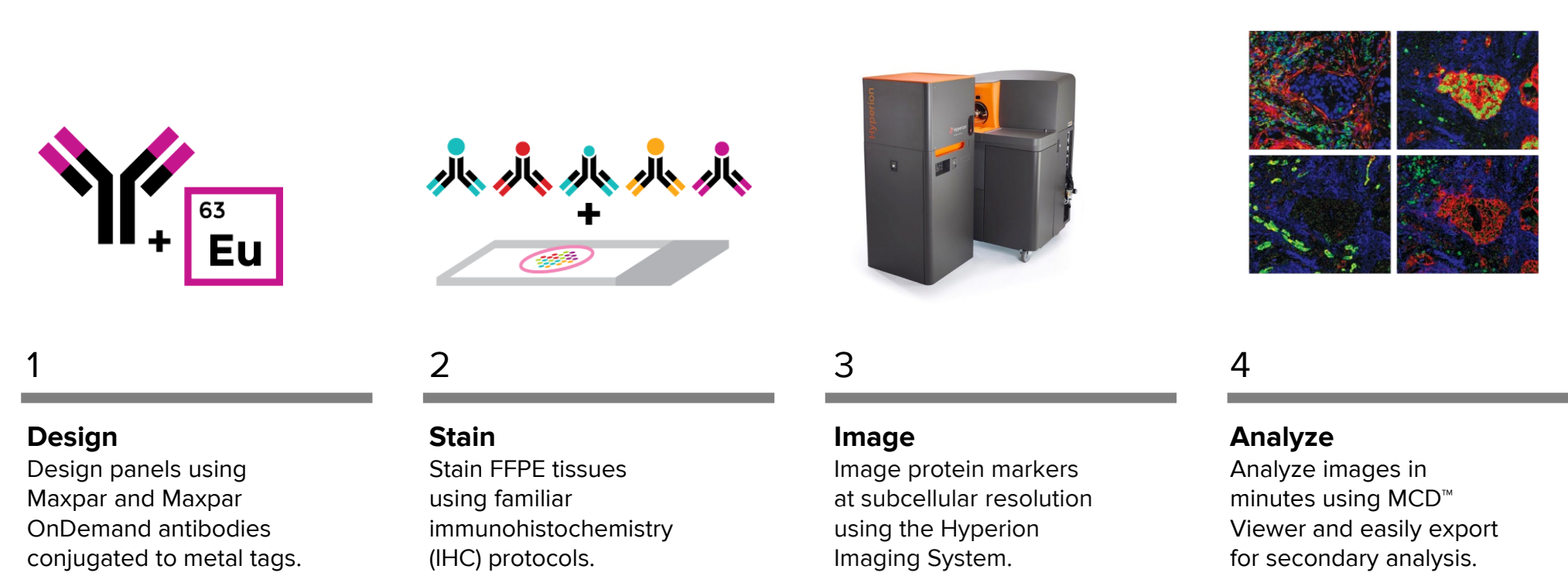
Introduction

Understanding cellular and structural composition of tissues can be highly composition through quantitative evaluation of selected cellular and structural tissue markers facilitates prediction of disease progression. Specifically, in preclinical models, changes in immune cell infiltration, adhesion state of epithelial cells, and composition of extracellular matrix in response to drug treatments are regularly probed using conventional techniques, yet these techniques require an excessive investment of time and resources. Imaging Mass Cytometry™ (IMC™) is a vital state-of-the-art tool to deeply characterize the complexity and diversity of any tissue without disrupting spatial context. The Hyperion™ Imaging System utilizes IMC, based on CyTOF® technology, to simultaneously assess up to 40 individual structural and functional markers in tissues on a single slide, providing unprecedented insight into the organization and function of the tissue microenvironment. We and others have previously demonstrated the application of IMC in combination with Maxpar® panel kits to highlight cellular composition of human tissues. Here, we showcase the recently released Maxpar OnDemand™ Antibodies for IMC application on mouse tissue. We introduced 11 additional methodically curated biomarkers to our existing mouse antibody catalog, providing the basis for the use of high-multiplex imaging in preclinical investigations.

Methods and Materials

To highlight the composition of the mouse tissue microenvironment, we applied IMC using a combination of Maxpar OnDemand and Maxpar catalog antibodies on normal mouse tissue microarrays (TMAs) containing a variety of normal FFPE tissues from major mouse organs such as lung, prostate, spleen, kidney, and more. Tissues were stained with a 20-marker panel designed to highlight tissue architecture and major immune lineage markers combined with our IMC Cell Segmentation Kit* (ICSK). The workflow summarized in Figure 1 was utilized to conduct staining, ablation, and downstream single-cell analysis to spatially resolve cellular and structural composition of normal mouse tissues.

Imaging Mass Cytometry workflow



Single-cell analysis workflow

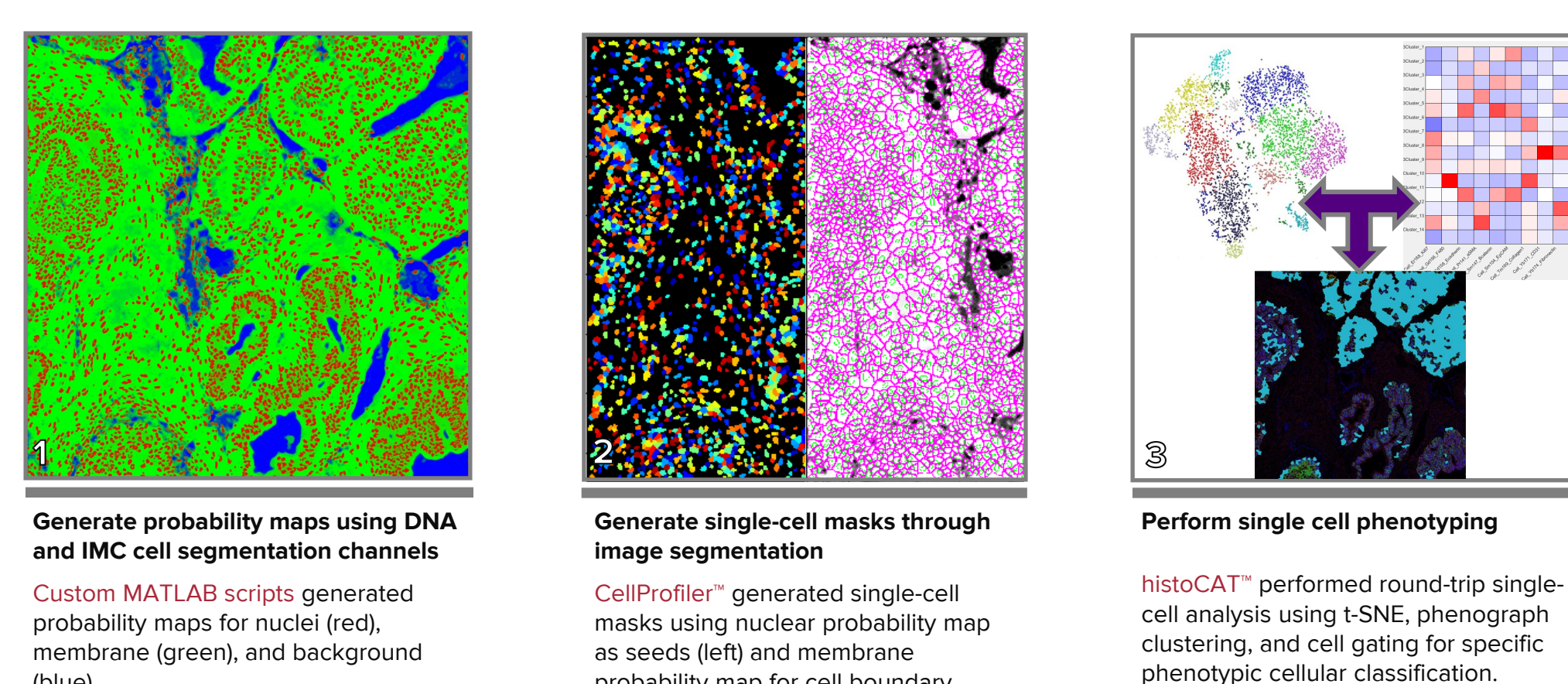


Figure 1. Imaging Mass Cytometry and single-cell analysis workflow. Normal mouse tissue was stained using a custom-designed panel of metal-conjugated antibodies to highlight specific cellular and structural markers. Stained tissues were ablated using Hyperion Imaging System at 200 Hz with 1 µm pixel size. Resulting images were rendered in MCD Viewer and exported for single-cell analysis. Probability maps for cell segmentation were generated using DNA channels and IMC cell segmentation kit which facilitates identification of cellular borders using plasma membrane markers that lead to improved nucleus and plasma membrane demarcation. Maps were imported to CellProfilr™ for single-cell segmentation and subsequently exported for single-cell phenotyping and cellular clustering to histoCAT. t-SNE maps and corresponding cell clusters were identified to assess relevant and highly specific cellular subpopulations.

Table 1. Antibody panel for IMC application on mouse FFPE tissue

No.	Marker Group	Target	Metal	Phenotype	Clone	Catalog No.
1	Immune cell markers	CD45	151Eu	Pan-immune immune cells	D3F8Q	91H029151
2		CD3	170Er	T cells	Polyclonal	31700919D
3		CD8	152Sm	Cytotoxic T cells	EPR21769	91H023152
4		CD4	162Dy	Helper T cells	BL1967	91H031662
5		F4/80	156Gd	Macrophage/granulocytes	D25SR	91H0301566
6		CD11b	149Sm	Myeloid cells	EPR1344	3149028D
7	Activated immune cell markers	INOS	164Dy	Immune cell differentiation	SP126	91H025164
8		FoxP3	165Ho	Regulatory T cells	FJK-16s	91H032165
9		Granzyme B	166Er	Activated NK and CTLs	EPR22645-206	91H026166
10	Epithelial cell markers	E-cadherin	158Cd	Epithelial cell-cell adhesion marker	24E10	3158023D
11		Beta-catenin	143Nd	Epithelial cell-cell adhesion marker	5H193	91H022147
12		EpCAM	154Sm	Epithelial cell-cell adhesion marker	EPR20532-222	91H024154
13	Vascular markers	alpha-SMA	141Pr	Smooth muscle cells	1A4	3141017D
14		CD31	171Yb	Endothelial marker	EPR17259	91H027171
15	Stromal markers	Fibronectin	174Yb	Extracellular matrix/fibroblasts	EPR19241-46	91H028174
16		Collagen I	169Tm	Extracellular matrix	Goat Poly	3169023D
17		Vimentin	143Nd	Fibroblasts	D2193	31430217D
18	Nuclear marker	Ki-67	158Er	Proliferating cells	B56	3158022D
19		DNA 1	191Ir	Cell-ID* Intercalator	-	201192A
20	Nuclear marker	DNA 2	193Ir	Cell-ID* Intercalator	-	201192A
21		ICSK 1	195Pt	Cell membrane marker 1	-	-
22	IMC Cell Segmentation Kit*	ICSK 2	196Pt	Cell membrane marker 2	-	-
23		ICSK 3	198Pt	Cell membrane marker 3	-	TIS-00001

* The IMC Cell Segmentation Kit is part of the Innovative Solutions menu of custom-made reagents and workflows developed and tested by Fluidigm scientists to give faster access to new cutting-edge solutions for high-multiplex single-cell analysis. Innovative Solutions are not part of the Maxpar catalog.

Results

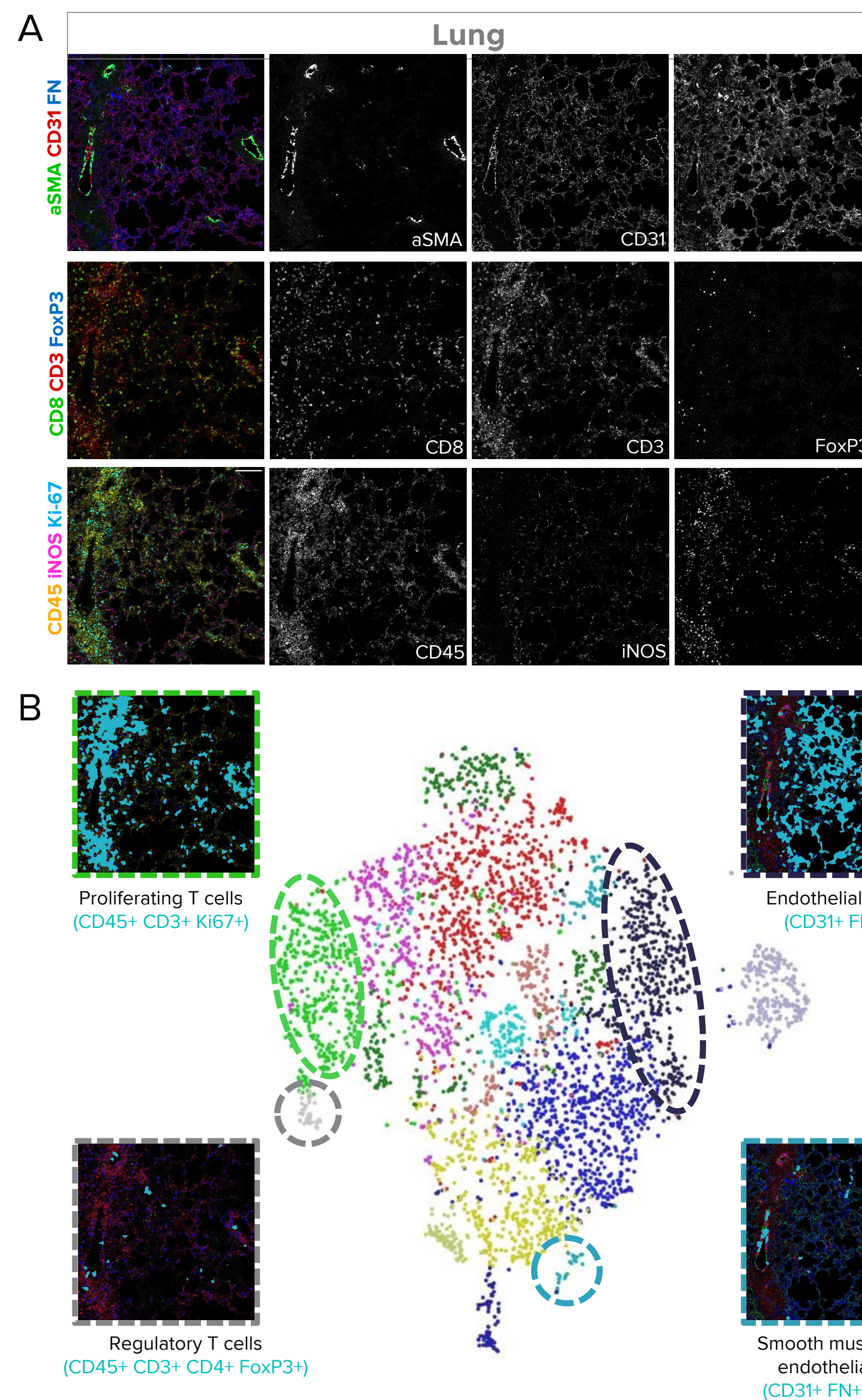


Figure 2. Composition of the normal mouse lung tissue microenvironment. (A) Representative multiplex and corresponding single-channel images demonstrate the localization of vascular cells, proliferating immune cells, and T cell subpopulations. (B) Single-cell analysis coupled with cell clustering identified 14 distinct clusters representing lung tissue microenvironment. Specific cellular populations such as capillary endothelial cells, smooth muscle-lined endothelial cells, and regulatory T cells were accurately identified. Full cluster list can be obtained in the supplementary material (QR code). Scale bar is 100 µm and is applicable to all images shown in A.

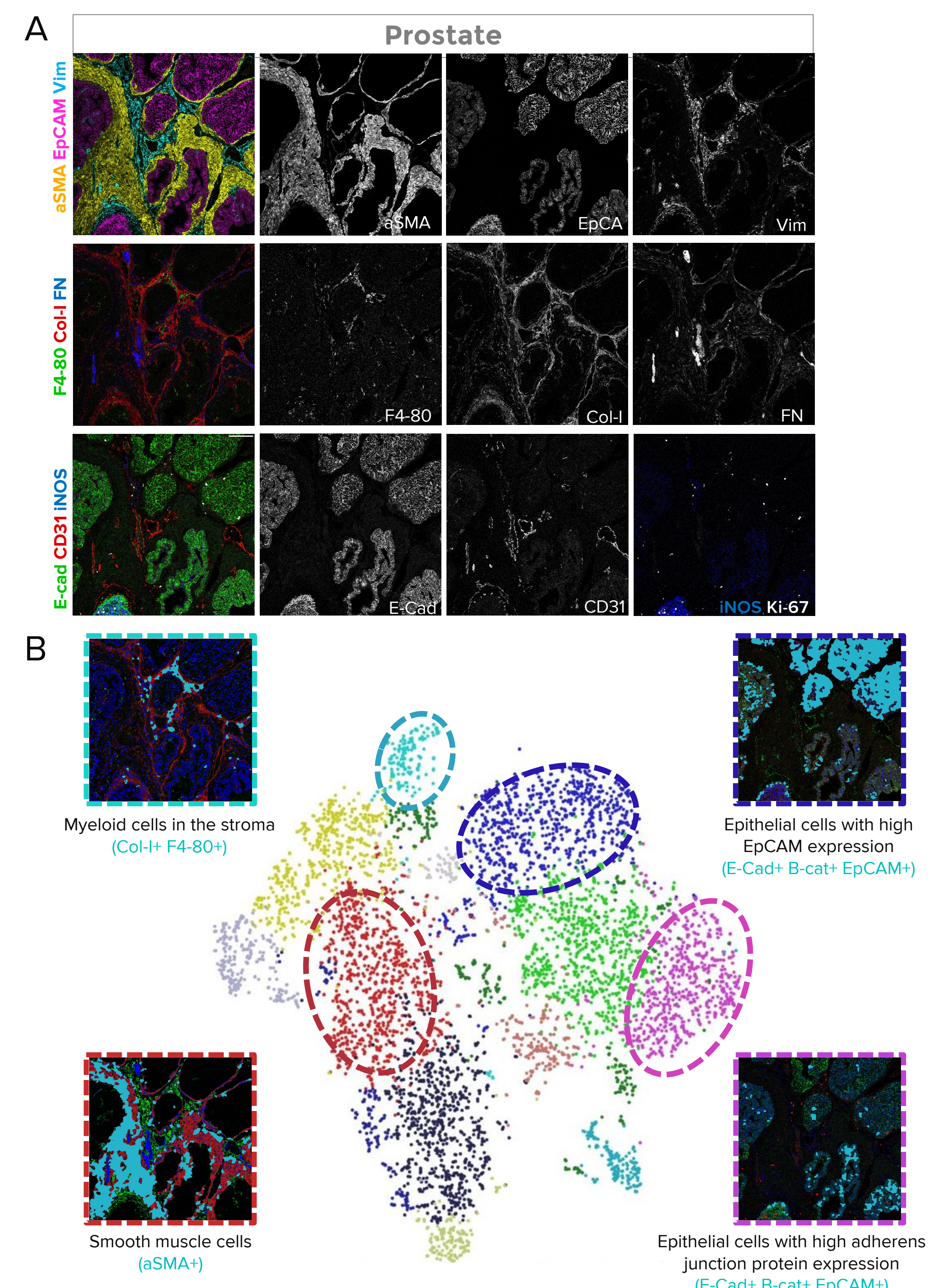


Figure 3. Composition of the normal mouse prostate tissue microenvironment. (A) Representative multiplex and corresponding single-channel images demonstrate the localization of epithelial, smooth muscle, and stromal cells, as well as myeloid cells, INOS-expressing epithelial cells, and the extracellular matrix components Col1 and FN. (B) Single-cell analysis coupled with cell clustering identified 14 distinct clusters representing prostate tissue microenvironment. Specific cellular populations such as subsets of epithelial cells and smooth muscle cells were accurately identified. Full cluster list can be obtained in the supplementary material (QR code). Scale bar is 100 µm and is applicable to all images shown in A.

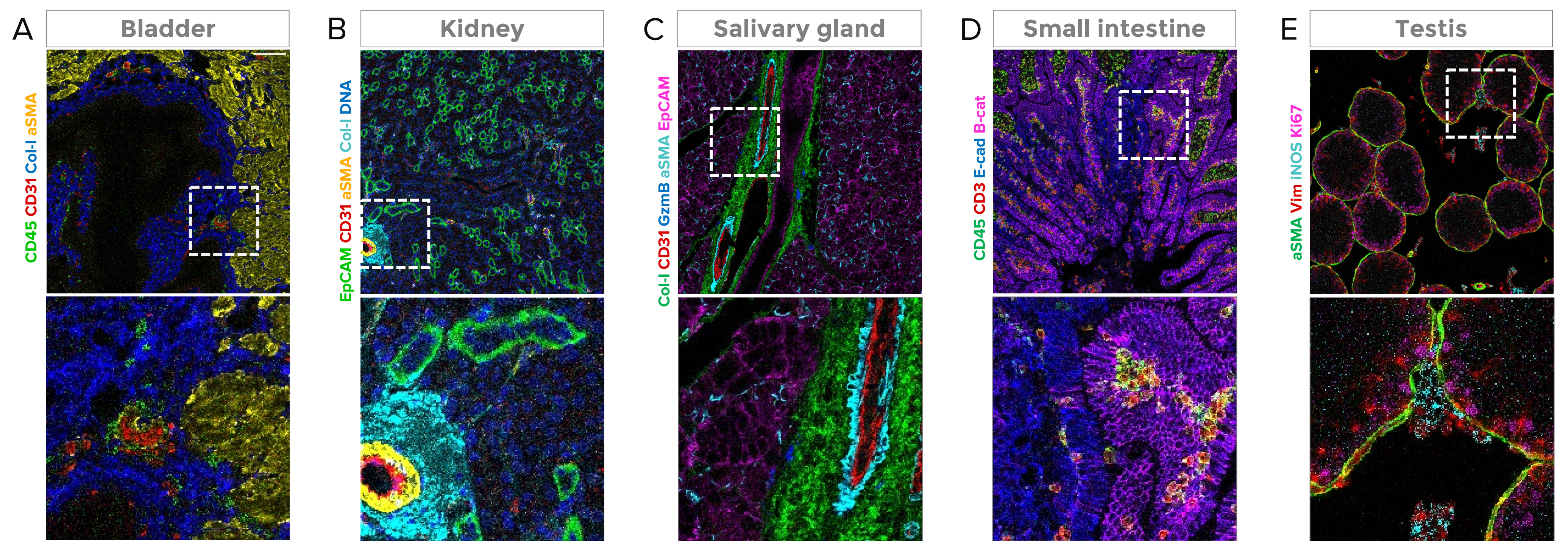


Figure 4. Localization of selected cellular markers in normal mouse tissue. (A) In the bladder, localization of CD45+ immune cells can be observed next to a CD31+ blood vessel. (B) In the kidney, ensheathment of a CD31+ blood vessel with aSMA+ smooth muscle cells and Col1-containing extracellular matrix can be observed. In addition, distal tubules are identified by high expression of EpCAM. (C) In the salivary gland, aSMA+ cells can be observed within the EpCAM+ epithelium. Additionally, large blood vessels embedded within Col1-rich extracellular matrix can be distinguished by the presence of CD31+ signal. (D) In the small intestine, localization of CD45+ immune cells and CD3+ T cells can be noticed in the lamina propria. E-cad+ epithelium with high or low expression of adapter protein B-cad can be observed. (E) In the testes, Ki67+ spermatogonia and Vim+ Sertoli cells can be identified in the aSMA+ outlined seminiferous tubules. INOS+ Leydig cells are present surrounding the seminiferous tubules. Scale bar is 100 µm and applies to all images except the insets.

Activation of immune cell

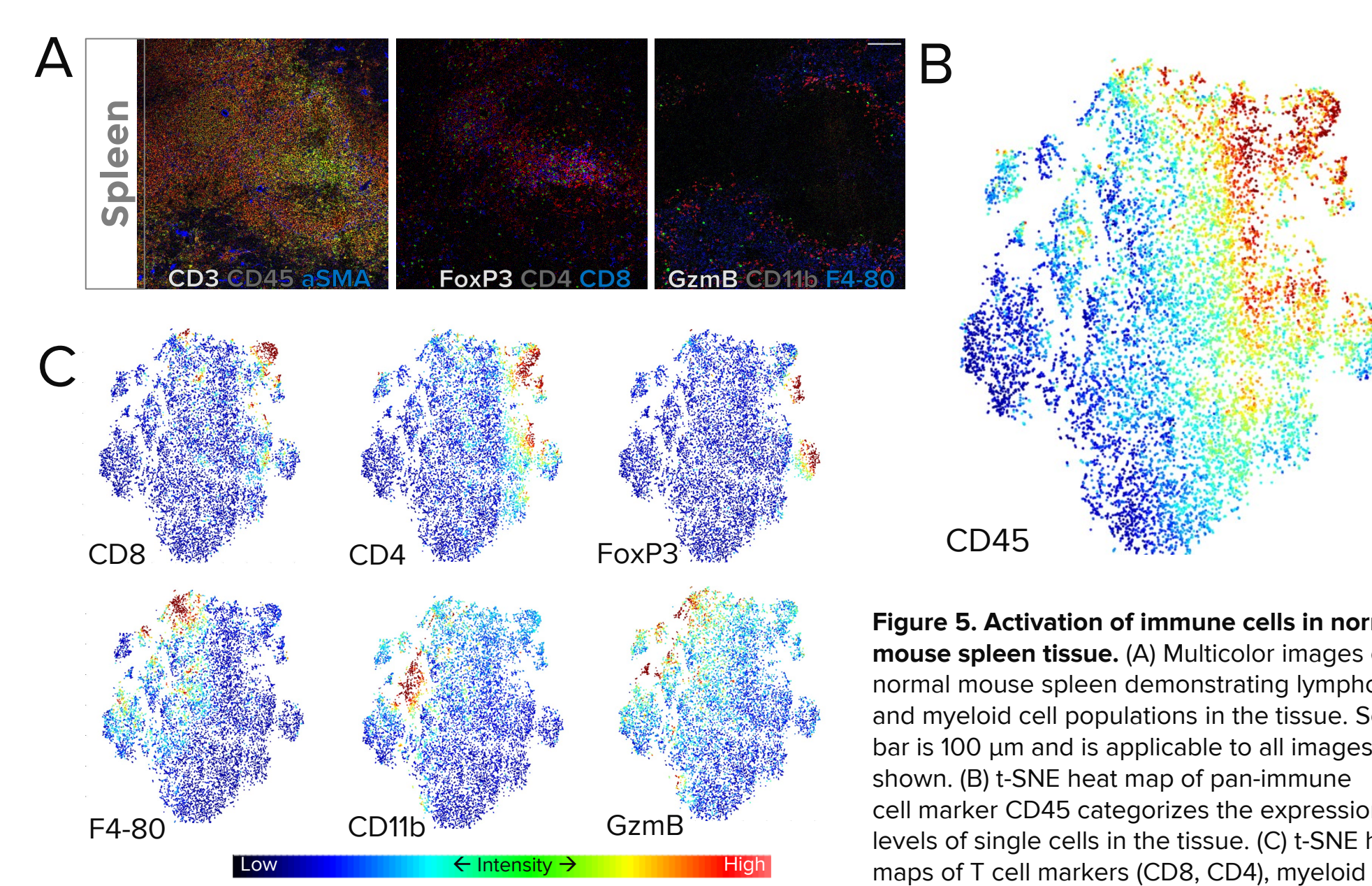


Figure 5. Activation of immune cells in normal mouse spleen tissue. (A) Multicolor images of normal mouse spleen demonstrating lymphoid and myeloid cell populations in the tissue. Scale bar is 100 µm and is applicable to all images shown. (B) t-SNE heat map of pan-immune cell marker CD45 categorizes the expression levels of single cells in the tissue. (C) t-SNE heat maps of T cell markers (CD8, CD4), myeloid cell markers (F4-80, CD11b), and immune cell activation markers (FoxP3, GzmB). Activated immune cell expressing, GzmB and FoxP3, can be identified in the plot and categorized as cytotoxic T cells (CD3+, CD8+, GzmB+), cytotoxic myeloid cells (F4-80+, GzmB+, CD11b+, GzmB+) and regulatory T cells (CD3+, CD4+, FoxP3+).

Cell-cell adhesion in epithelial cells

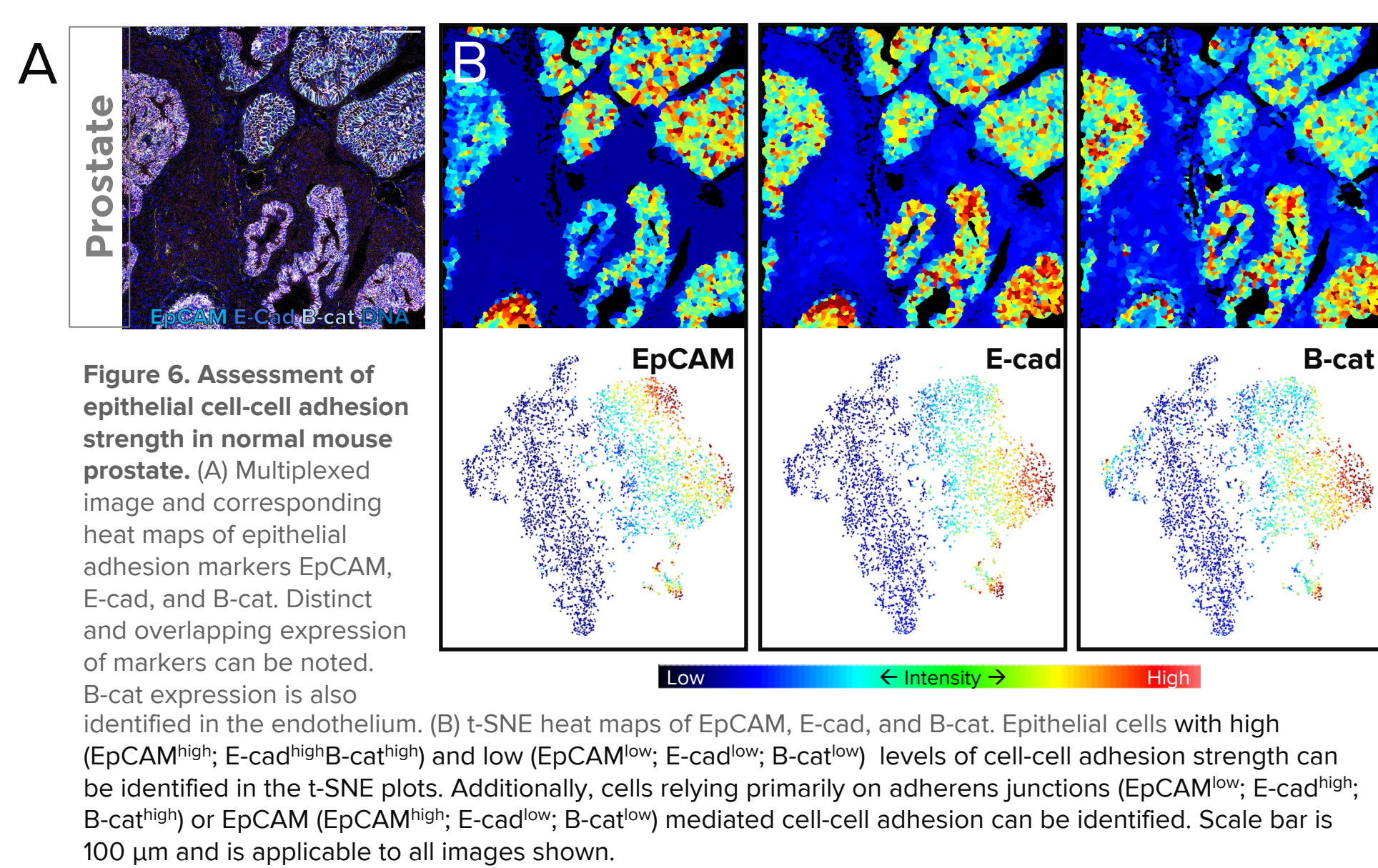


Figure 6. Assessment of epithelial cell-cell adhesion strengths in normal mouse prostate. (A) Multiplexed image and corresponding heat maps of epithelial adhesion markers EpCAM, E-cad, and B-cad. Distinct and overlapping expression of markers can be noted. B-cad expression is also identified in the endothelium. (B) t-SNE heat maps of EpCAM, E-cad, and B-cad. Epithelial cells with high (EpCAM^{high}, E-cad^{high}, B-cad^{high}) and low (EpCAM^{low}, E-cad^{low}, B-cad^{low}) levels of cell-cell adhesion strength can be identified in the t-SNE plots. Additionally, cells relying primarily on adherens junctions (EpCAM^{high}, E-cad^{high}, B-cad^{low}) or EpCAM (EpCAM^{high}, E-cad^{low}, B-cad^{low}) mediated cell-cell adhesion can be identified. Scale bar is 100 µm and is applicable to all images shown.

Extracellular matrix composition

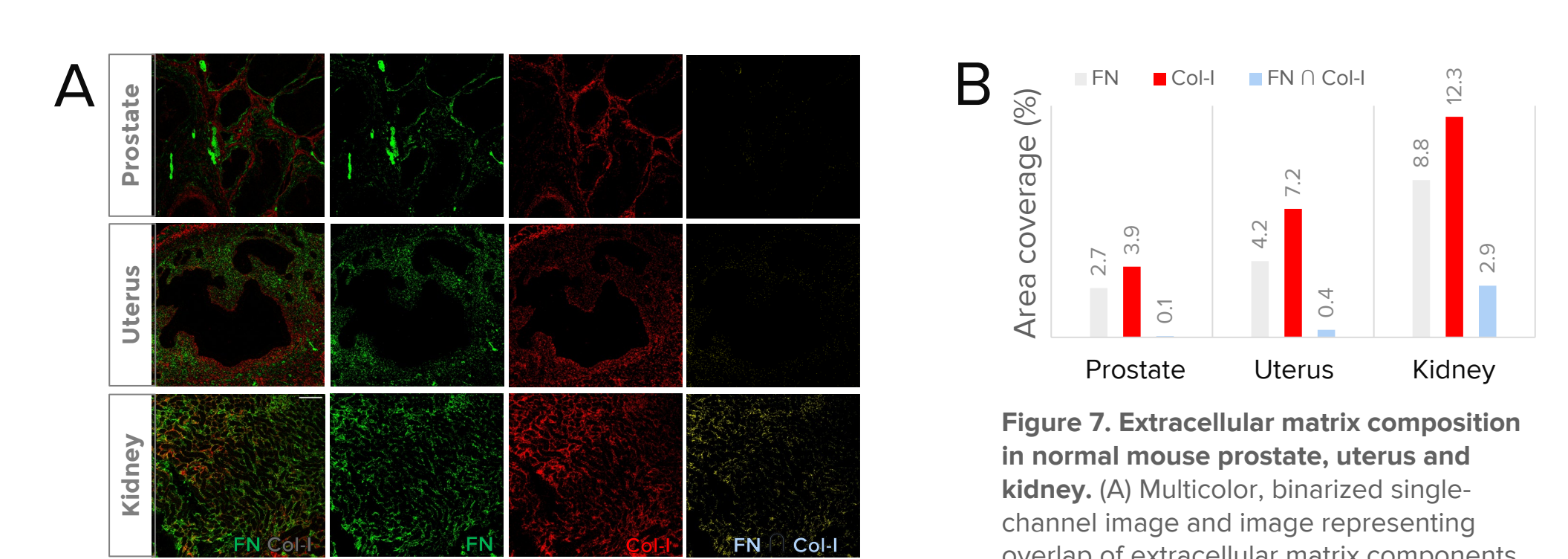


Figure 7. Extracellular matrix composition in normal mouse prostate, uterus and kidney. (A) Multicolor, binarized single-channel image and image representing overlap of extracellular matrix components FN and Col1 are shown. (B) Quantification of extracellular matrix containing FN, Col1, and their overlap. In prostate and uterus, FN and Col1-containing extracellular matrix occupies largely distinct areas of the tissue. In kidney, extracellular matrix area containing both FN and Col1 can be readily identified. Scale bar is 100 µm and is applicable to all images shown.

Conclusions

- Generated a marker panel to highlight key characteristics of the mouse tissue microenvironment such as immune, epithelial, and stromal cell populations
- Demonstrated the performance of 11 new mouse-specific IMC antibodies available through Maxpar OnDemand with multiple metal combinations for ease of panel design
- Determined the localization of lymphoid and myeloid cell subpopulations through application of single-cell analysis on 23-marker images with 1 µm pixel size
- Identified activation of lymphoid and myeloid cells, assessed the strength of cell-cell adhesion in epithelial cells, and revealed the composition of the extracellular matrix
- The analysis presented here demonstrates the capability of the IMC technology to identify subcellular localization of cellular and structural markers, providing the basis for the use of high-multiplex imaging in preclinical investigations related to immuno-oncology applications.

